JOURNAL OF MATERIALS SCIENCE 24 (1989) 523–535

Plastic flow and fracture of $Pd_{40}Ni_{40}P_{20}$ metallic glass under an indentor

P. E. DONOVAN
Department of Materials Science and Metallurgy, University of Cambridge, Pembroke Street, Cambridge, UK

The geometry of plastic flow under spherical and Vickers indentors in $Pd_{40}Ni_{40}P_{20}$ metallic glass has been investigated by sectioning and etching. The surface pile-ups and slip lines around the indentations are found to be only a small part of the total deformation. Beneath the surface extensive plastic zones are formed in which material is moved radially away from the indentor, but this movement is produced by slip on surfaces of high shear stress rather than by direct radial flow or compaction. Networks of cracks or incipient cracks also form around an indentation but are not normally visible until the material is etched.

1. Introduction

The Vickers hardness test is probably the mechanical test most commonly applied to metallic glasses because it is quick, easy to perform and can be carried out on relatively rough, thin, melt-spun ribbons. It is routinely used to assess quenching rates, embrittlement and crystallization or to obtain information about the chemical bonding (e.g. [1]). Metallic glasses are generally highly ductile materials and therefore a hardness test produces a well-defined plastic indent which is usually surrounded by "coronets" of slip bands in which material is piled up along the faces of the indentor [2]. However, two other indent morphologies have been reported. In some cases, for example on annealing $Fe_{40}Ni_{40}P_{14}B_6$ metallic glass, the tendency to produce coronets is suppressed [3] and no slip lines or other features can be seen in the region around the indent, while in other cases, particularly at low temperatures [4] or in partially crystallized glasses, radial markings are produced around the plastic indentation which have been inferred, but not proved, to be cracks. These changes in indent appearance have not been explained.

Metallic glasses should be good model materials for testing theories of indentation plasticity because they are isotropic and do not work-harden, and they are thus a close approximation to ideal elastic/plastic solids even though their slip planes are not always precisely the planes of maximum resolved shear stress [5]. The aim of this investigation was to make a detailed comparison between the patterns of slip produced experimentally by indentation of a metallic glass, the patterns of flow which have been reported for other materials and the predictions of the available theories, in an attempt to determine, firstly, the factors which control the geometry of plastic flow around an indentation in metallic glasses and, secondly, whether their mechanism of flow has an identifiable effect on the behaviour.

2. Indentation plasticity and fracture

2.1. Ductile materials

Isotropic materials which deform plastically under an indentor fall into one of three classes [6]. If the elastic deformation is negligible, i.e. the ratio of Young's modulus, E, to the hardness pressure, H, is large, the behaviour in the absence of work-hardening approaches that of an ideal rigid/plastic solid and slip-line field theory predicts that the displaced material flows up around the indentor to form a raised "pile-up". This flow pattern is observed in fully work-hardened crystalline metals. Under these circumstances H will be proportional to the uniaxial compressive yield stress, Y, and the constant of proportionality is predicted to be about 3. If, on the other hand, E/H is small, a substantial part of the applied load will be supported by elastic compression and most of the displacements will be radial, although some piling up is still expected to occur around a sharp indentor. This behaviour is described by the "expanding spherical cavity" model applied by Marsh to the indentation of silicate glasses [7]. On this model the relationship between H and Y for a spherical indentor is predicted to be

$$H/Y = 2(1 + \ln\{E/[3(1 - \nu)Y]\})/3 \quad (1)$$

where ν is Poisson's ratio. The third class of behaviour is that of well-annealed crystalline metals, where rapid work-hardening leads to sinking-in of material adjacent to the zone of contact with the indentor.

2.2. Brittle materials

If a material is brittle, fracture as well as plastic flow may occur during indentation. The pattern of cracking observed is dependent on the shape of the indentor, the load applied and the material being tested. Beneath a pointed indentor the "standard" crack pattern consists of one or more "median" cracks, which form during loading and propagate normal to the

0022–2461/89 $03.00 + .12

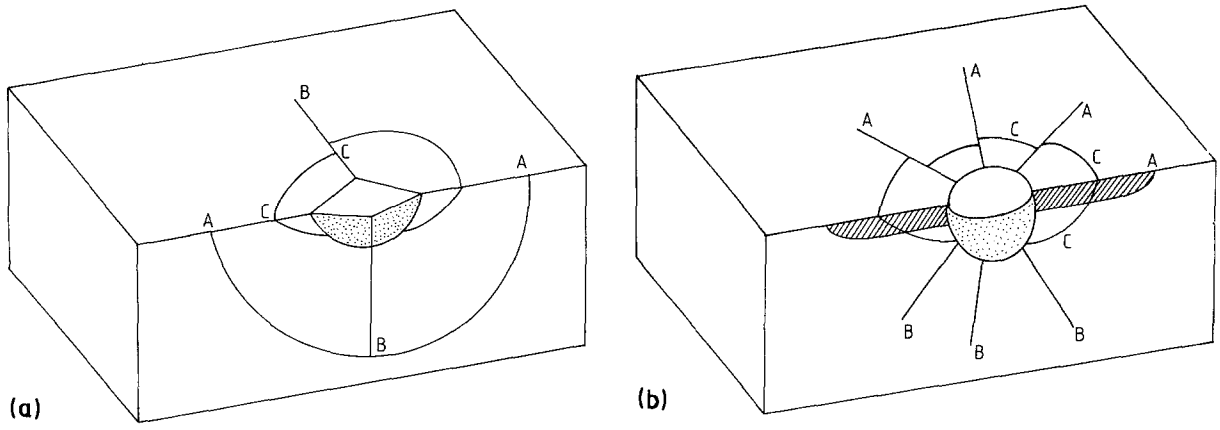

Figure 1 Diagrams illustrating the usual crack patterns around indentations in brittle materials: (a) Vickers indentation, with penny-shaped median cracks A–B–A and B–B, lateral cracks C and plastic zone (stippled); (b) spherical indentation, with shallow radial cracks A, deep radial cracks B, lateral cracks C and plastic zone.

surface, together with a system of saucer-shaped "lateral" cracks which run up from the plastic zone towards the surface and are formed by the residual stress field as the specimen is unloaded [8]. This crack pattern is illustrated schematically in Fig. 1a. In some materials a third system of relatively shallow radial cracks ("Palmqvist cracks") is also formed around the plastic zone. Fig. 1b illustrates the related systems of radial and lateral cracks formed under a blunt, spherical indentor. In very brittle solids such as soda–lime glasses a Hertzian cone crack may also develop under a spherical indentor [9]. The extensive literature on the crack patterns obtained by the indentation of brittle solids has recently been reviewed by Ostojic and McPherson [10].

2.3. Metallic glasses

Metallic glasses are highly ductile and undergo no work-hardening during a uniaxial test, so their behaviour on indentation would be expected to agree with the predictions of either slip-line field theory or the expanding cavity model. In an earlier paper [11] it was pointed out that the values of E/H for metallic glasses are small (less than 20) and that they would therefore be expected to follow the expanding cavity model, but that the coronets observed around the indents suggest that the displacements are directed towards the surface, as predicted by slip-line field theory, rather than in a radial direction. The observed behaviour thus seems not to be in agreement with the standard models of indentation plasticity, and it was suggested that a possible explanation for this might lie in the mechanism of plastic flow.

At room temperature metallic glasses undergo some viscous flow, in which strain is continuously distributed throughout the material, but almost all the plastic strain is concentrated in narrow, highly localized "shear bands". The development and operation of these bands is thought to be due to dilatation of the deforming material [12, 13]. Experiments have shown that the yield strength of a metallic glass depends on the perpendicular stress on the slip plane, i.e. the glass obeys a Mohr–Coulomb yield criterion of the form

$$t_y = t_0 + \alpha\sigma_n \qquad (2)$$

where t_y is the shear yield stress, t_0 is the yield stress in pure shear, σ_n is the normal stress on the slip plane and α is a constant [10]. Plastic flow is thus easier when σ_n is negative (tensile) than when it is compressive. It was suggested [11] that the surface-directed slip producing the coronets might occur in spite of a low value of E/H because plastic flow is promoted by the tensile stresses parallel to the surface around the loaded indentor while radially-directed slip is inhibited by the high sub-surface compressive stress. Examination of the flow patterns produced beneath the surface during indentation should show whether this tentative explanation is correct, because such an effect should lead to appreciable distortion of the shape of the plastic zone.

Most metallic glasses can only be produced as thin films or as melt-spun ribbons up to about 50 μm thick. For valid indentation testing the indent depth must be less than one-tenth of the specimen thickness; if the indent is deeper than this the proximity of the lower free surface distorts the stress field [6]. Indentations in metallic glass ribbons must therefore be relatively small and this makes it difficult to observe the plastic zone in any detail. However, certain palladium-based glasses can be prepared at low cooling rates in sections up to 2 mm thick [14]. This investigation has been performed on one of these glasses, $Pd_{40}Ni_{40}P_{20}$. This has the advantage that the elastic constants [15, 16] and compressive yield strength of this glass have been measured, and these are shown in Table I.

3. Experimental procedure

Cylindrical specimens of $Pd_{40}Ni_{40}P_{20}$ glass up to 2 mm in diameter were prepared by quenching the alloy in drawn silica tubes, as described elsewhere [5]. The ends of the cylinders were ground flat and parallel and the end which was to be indented was polished to 1 μm finish with diamond polish. Vickers indentation tests were carried out in a standard testing machine at loads up to 10 kg. Spherical indentation testing was carried

TABLE I Elastic and plastic properties of $Pd_{40}Ni_{40}P_{20}$

Young's modulus	108 GPa [21]
Poisson's ratio	0.40 [21]
Shear modulus	40.6 GPa [21]
Bulk modulus	185 GPa [21]
Uniaxial compressive yield strength	1.78 GPa [10]
α (Equation 2)	0.11 [10]

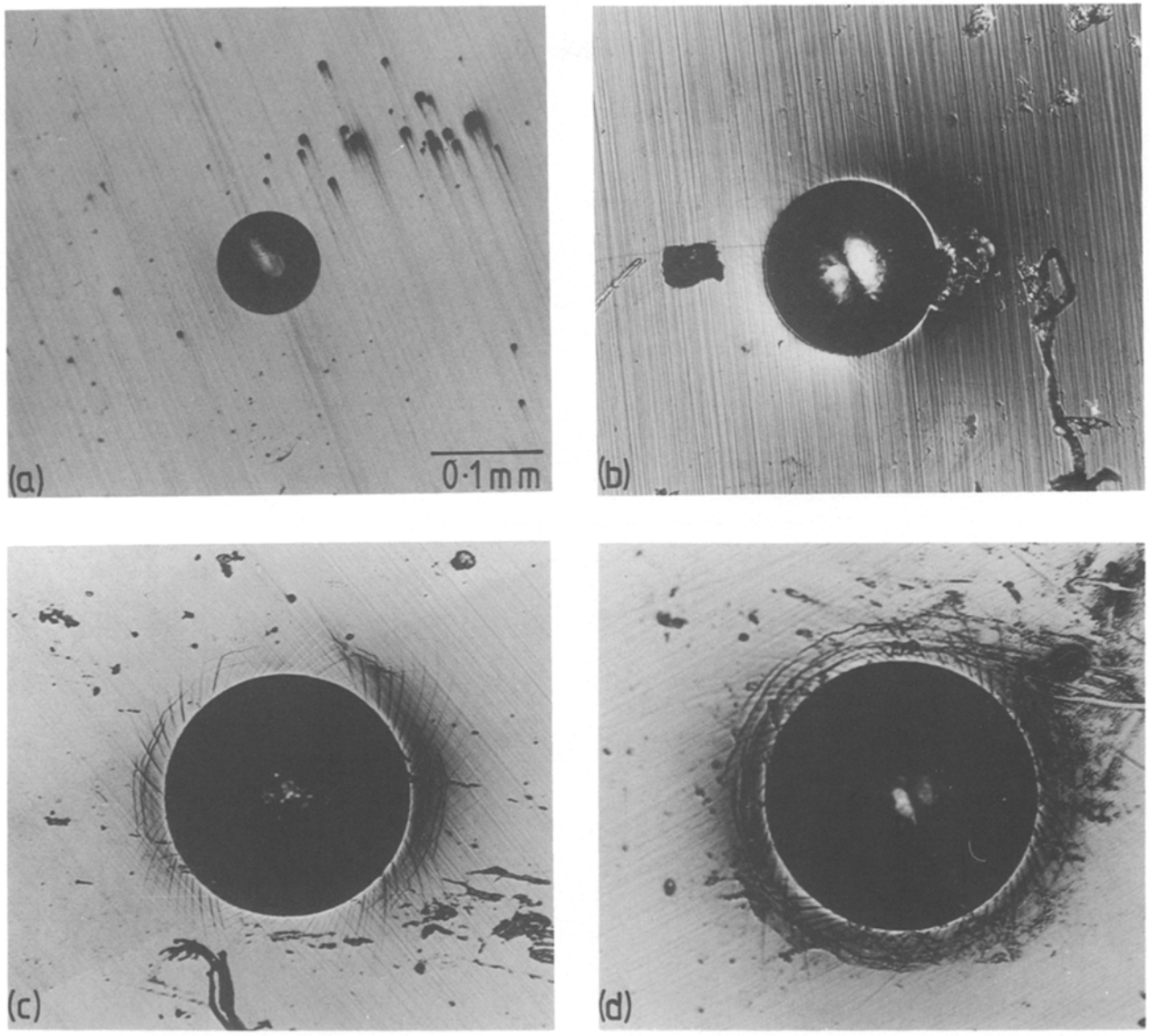

Figure 2 Spherical indentations produced at different loads: (a) 0.05 kN, (b) 0.14 kN, (c) 0.20 kN, (d) 0.29 kN. Nomarski interference contrast.

out in a servohydraulic testing machine supplied by ESH Testing Limited, operating at a constant displacement rate of 1 μm sec^{-1}. The indentations were made with precision-machined 0.4 mm diameter tungsten carbide balls, the specimen and the ball being squashed together between hardened steel platens until the desired load was reached.

The deformed specimens were examined by light microscopy and in the scanning electron microscope (SEM). Specimens were etched to reveal the plastic zone in a solution of three parts HCl, one part HNO_3 and two parts H_2O (aqua regia) for 4 min. Some of the specimens were mounted in resin and sectioned by grinding on 1200 grit paper followed by polishing to 1 μm finish in the usual way. Sections through the indentations were prepared in two orientations: "horizontal" sections parallel to the original surface of the specimen and "vertical" sections perpendicular to the original surface.

4. Spherical indentations

Indentations were made at a range of loads to determine the approximate form of the stress–strain curve in the plastic region [6]. The results of the tests are shown in Table II. It can be seen that to within the accuracy of the experiments, which is mainly limited by the accuracy with which the indentation diameter can be measured, the glass does not work-harden even at high plastic strains. This is in agreement with the results of uniaxial compression tests on this material [5].

The average value of the hardness, H_S, obtained by dividing the applied load by the projected area of the indent, is $551 \pm 72\,\mathrm{kg\,mm^{-2}}$. This is comparable to the value of $540\,\mathrm{kg\,mm^{-2}}$ obtained by Davis *et al.* [16] for the Vickers hardness of this glass and it is approximately equal to three times the compressive yield stress given in Table I. This value of 3 is in agreement with the predictions of both the expanding cavity model (Equation 1), which predicts $H/Y = 3.01$, and the slip-line field model.

The changes in appearance of the indents as the applied load is increased are shown in Fig. 2. At the lowest loads applied (< 0.1 kN) there are no coronets or other visible features around the indent and interference microscopy reveals no changes in height of the surface. At higher loads spiral slip lines begin to appear on the surface, as described by Hartmann [17], and at even higher loads (~ 0.2 kN) sections of coronet pile-up appear, as shown in Fig. 2c, which

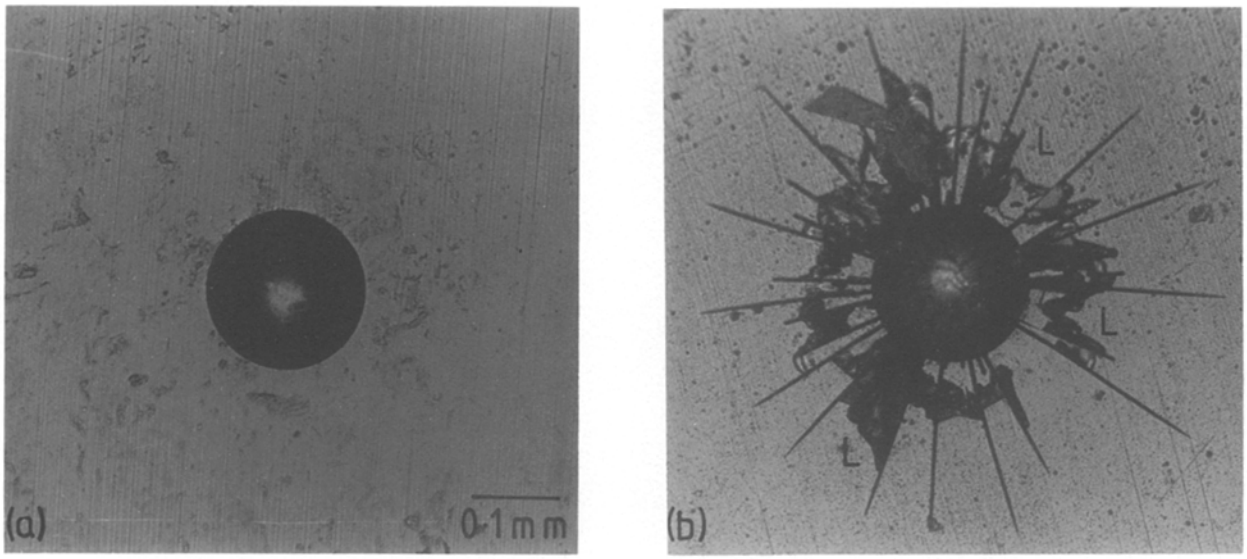

Figure 3 Spherical indentation (a) before and (b) after etching in aqua regia.

eventually extend symmetrically around the indentation. Even at the highest load applied in this investigation, which corresponds to a very large local plastic strain ($a/R = 0.74$), there is no sign of crack-formation either in or around the indentations.

However, when the specimen is etched a very different picture emerges. This is illustrated in Fig. 3, which shows the surface appearance of the same indentation before and after etching. The acid reveals a well-developed system of radial cracks, extending out to a distance of the order of three indent radii. These cracks were observed after etching in all the specimens tested, although their number and length increased with the applied load. At loads greater than 0.05 kN shallow lateral cracks were also observed. Some of these are labelled "L" in Fig. 3b.

Some details of the radial and lateral cracks are shown in Fig. 4. It can be seen that the radial cracks are of several different lengths. Some of them extend outwards well beyond the zone of surface plasticity marked by the Hartmann lines but others terminate at about the elastic/plastic boundary. They also extend inwards by different amounts, some of them running right into the contact area. The radial cracks are arranged approximately symmetrically around the indent but the long, well-developed cracks are rarely exactly opposite one another and thus cannot be the surface traces of the penny-shaped median cracks illustrated in Fig. 1a. The lateral cracks form saucer-shaped segments between pairs of radial cracks and the distance between the point where they reach the surface and the centre of the indent is often quite different for adjacent segments, as can be seen in Fig. 4a.

TABLE II Spherical indentations in $Pd_{40}Ni_{40}P_{20}$

Load (kN)	Indent diameter (mm)	Indent radius/ Indentor radius (mm)	H_v (kg mm^{-2})
0.359	0.292	0.736	5.36 ± 0.07
0.290	0.259	0.652	5.51 ± 0.09
0.250	0.245	0.617	5.30 ± 0.10
0.201	0.222	0.559	5.19 ± 0.10
0.200	0.223	0.562	5.12 ± 0.10
0.151	0.200	0.504	4.81 ± 0.12
0.140	0.183	0.461	5.32 ± 0.12
0.101	0.162	0.408	4.90 ± 0.15
0.100	0.157	0.395	5.17 ± 0.18
0.050	0.095	0.239	7.07 ± 0.95
0.030	0.074	0.187	6.90 ± 1.00

Development of the lateral cracks in the etch leads to movement of the surface. Fig. 4b shows how the material above the lateral cracks moves upwards and inwards; if etching is prolonged the chip of material may be completely removed. It should be recalled that absolutely no vertical displacement of the surface could be detected before etching, which indicates either that lateral cracks were present but did not extend as far as the surface or that they were present in the form of crack nuclei or incipient cracks which were opened up in the etch by stress-corrosion. The radial cracks, once developed, are well-defned. The etch penetrates deeply along them, as illustrated in Fig. 4c, and they do not change their length or shape even on prolonged further etching. Development of the radial cracks by etching leads to no detectable surface movements.

Some evidence that radial cracks are present but do not extend as far as the surface before etching is shown in Fig. 5. For this indentation the pattern of cracks observed after etching was unusually asymmetric, with one abnormally long radial crack, labelled "A" in Fig. 5a, and another radial crack which would be required to complete the pattern at "B" absent. Fig. 5 shows a progressive series of horizontal sections through this indent, and it can be seen in Fig. 5e that the missing crack at "B" is, in fact, present beneath the surface. Many short sections of crack at the boundary of the plastic zone which run approximately parallel to the main radial cracks are also only visible on sub-surface sections. All the cracks revealed beneath the original surface on horizontal sections have radial traces: there is no evidence for circumferential "ring" cracking.

The sections in Fig. 5 also show the plastic zone.

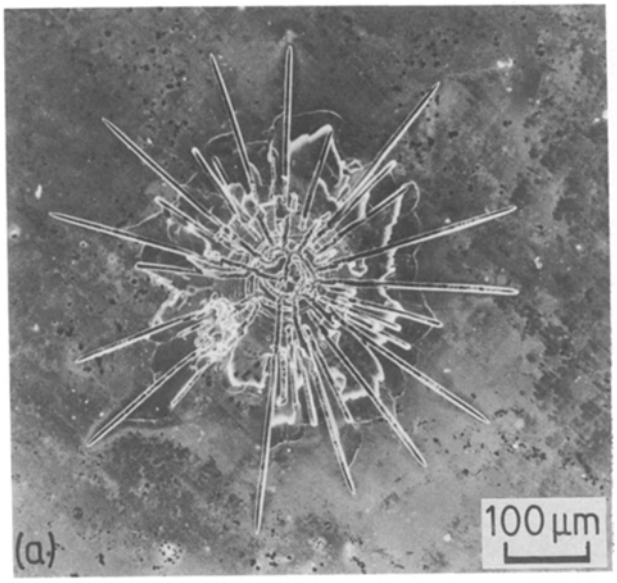

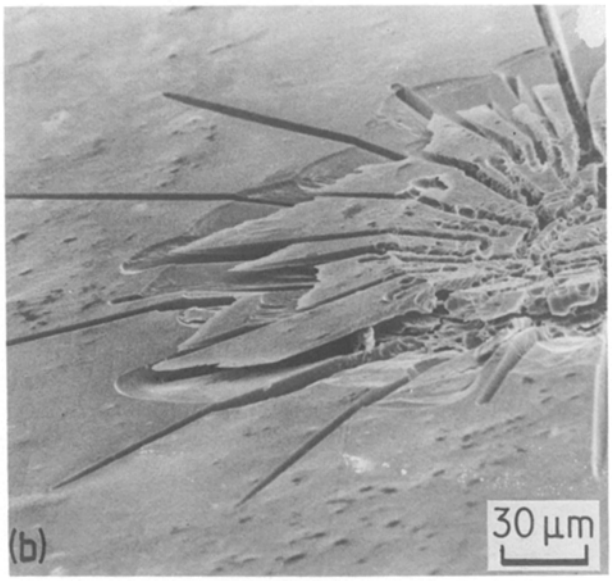

Figure 4 SEM images of an etched spherical indentation.

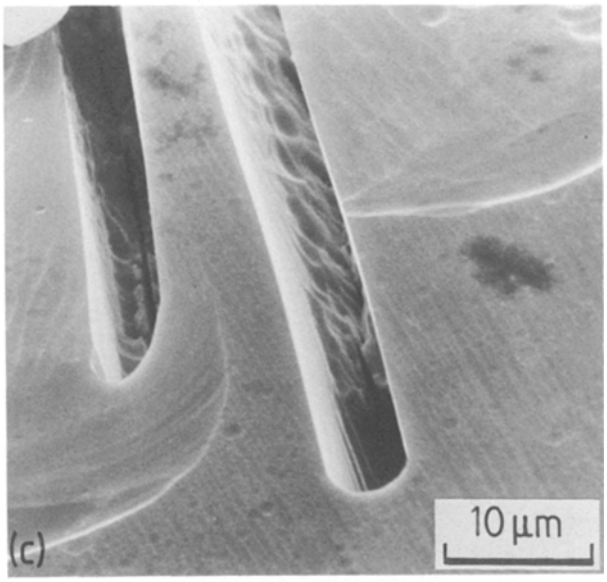

The shear bands are etched lightly by the acid and show up as faint lines when the specimen is imaged in interference contrast with a Nomarski phase plate. Unfortunately, the 1 μm polishing scratches also show up in interference contrast, but attempts to remove the scratches by electropolishing before etching produced a bumpy surface which obscured the height changes at the etched bands. As a compromise the specimens were held during polishing so that the scratches were straight, which allows them to be distinguished in the images from the curved shear bands.

The extended zone of surface plasticity associated with the Hartmann lines is shallow. Immediately below the surface, around the indentor contact zone, the plastic zone does not extend very far in the radial direction and those slip lines which can be resolved near the edge of the plastic zone appear as short, circumferential line segments. However, as the distance of the plane of the section from the original surface increases spiral lines coming out from the centre can also be seen (Fig. 5c) and as the depth increases further, the tight circular plastic zone spreads out and becomes more diffuse and the proportion of spiral slip line traces increases until eventually (Fig. 5f) only spiral lines remain. The lateral cracks and the parts of the radial cracks which extend right into the contact zone are also extremely shallow: on sub-surface sections no lateral cracks appear and the inner ends of the radial cracks closely follow the boundary of the plastic zone. In Fig. 5b a root crack can be seen at the centre of the indentation, but this also appears to be shallow.

From Fig. 5 it is evident that the plastic zone extends to a much greater depth than the radial cracks. This is confirmed by Fig. 6, which shows a similar set of horizontal sections through an indentation produced at a lower load than the one shown in Fig. 5. Although a complete set of shallow surface lateral and radial cracks would have been produced at this load, sectioning reveals only one deeper radial crack. It may be significant that this is also the load (0.2 kN) at which incomplete circumferential pile-ups are first observed at the free surface.

When an indentation is sectioned in a vertical plane, once again no cracking is observed before etching, as illustrated in Fig. 7a. However, etching again reveals a well-defined system of subsurface cracks as well as the plastic zone. Considering the plastic zone first, it can be seen immediately from Fig. 7b that surface features such as the circumferential pile-ups represent a very small part of the deformation. The shape of the plastic zone can be described as part of a sphere with its centre about two to three times the indent depth below the free surface. The plastic zone has a core region immediately beneath the contact zone in which individual slip lines cannot be distinguished, but intersecting spiral slip lines emanate from this core and propagate outwards into the elastic region, in most cases to terminate within the specimen although a very few reach the surface. The Hartmann surface slip lines are observed to follow curved planes beneath the surface, as shown in Fig. 7c.

The crack distribution shown in Fig. 7b is predominantly radial, resembling the radial cracking observed beneath spherical indentations in other materials [18],

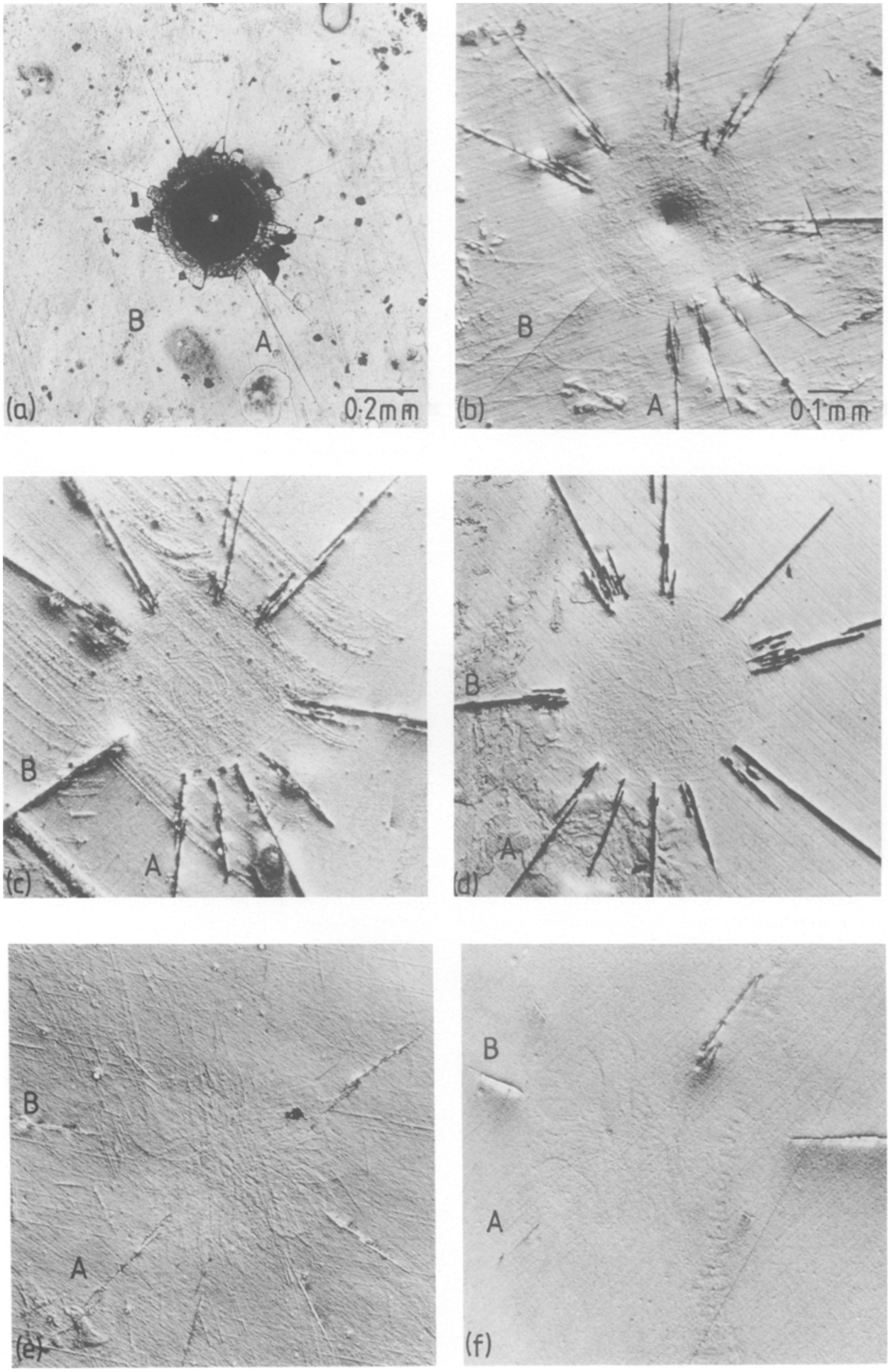

Figure 5 Horizontal sections through a spherical indentation. (a) The original surface, (b) to (f) sections at increasing depth. Corresponding points are labelled on each picture. Nomarski interference contrast.

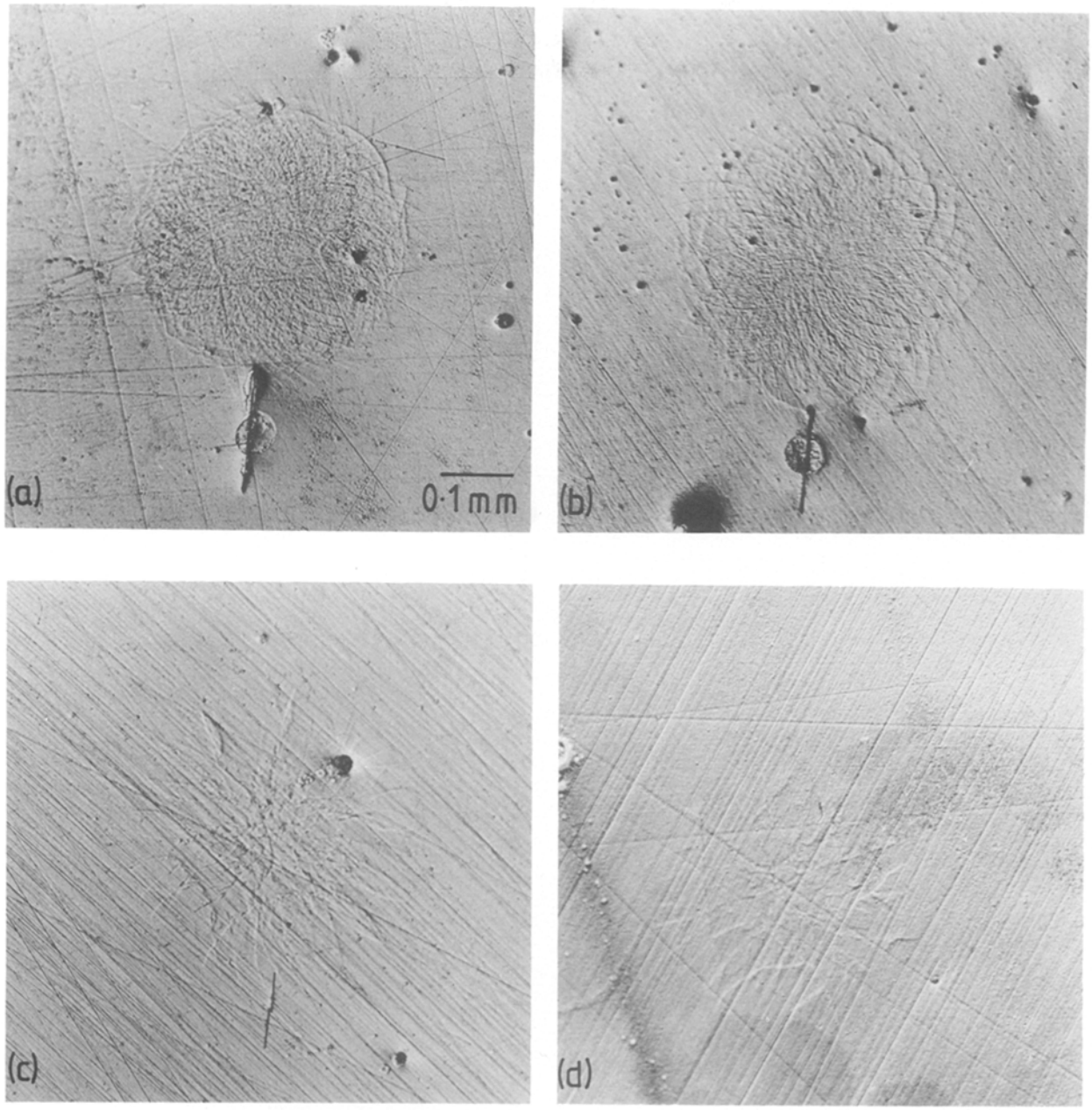

Figure 6 Horizontal sections through a spherical indentation, showing the shallowness of the radial cracks and the changing shape of the plastic zone. Nomarski interference contrast.

but some of the main cracks appear to pass right through the core of the plastic zone, unlike the crack traces seen on the horizontal sections in Figs 5 and 6. However, this appearance is deceptive. It arises because Fig. 7b is a section near to the edge of the indent rather than through its centre. A subsequent section closer to the centre of the indentation is shown in Fig. 7d and this clearly demonstrates that these cracks also approximately follow the edge of the plastic zone. Although the slip lines have not etched up in Fig. 7d, the position of the edge of the plastic zone can be seen as a deflection of the line of the cracks away from the free surface as at the point labelled "Z". Presumably these cracks started at the edge of the plastic zone when it was a little smaller, because new cracks, for example at point "B", now appear to be starting from the present position of the elastic/plastic boundary. Careful examination of series of vertical sections like the one shown in Fig. 7 suggests that the subsurface "radial" cracks actually lie on approximately conical surfaces. The apex of each cone crack lies at the base of the "core" of the plastic zone and from this point a set of co-axial conical cracks slants upwards and downwards, appearing as parabolae on sections such as Fig. 7b. However, each crack does not form a complete cone, like the Hertzian cone cracks in silicate glasses [18], instead only parts of each conical surface are cracked. The cracking is most developed outside the plastic zone; within the central core no cracks are observed at all and on sections close to the central symmetry plane of the indentation relatively few traces of the cone cracks appear.

Fig. 7b also shows the traces of some of the shallow radial cracks within the contact zone. On etching, these contact zone cracks may link up with the subsurface crack system, as shown in Fig. 8. The surface of this specimen, unlike that shown in Fig. 7, was etched before vertical sectioning, so the relative depths of the surface and sub-surface crack systems can be seen. Closer to the central section through this indent

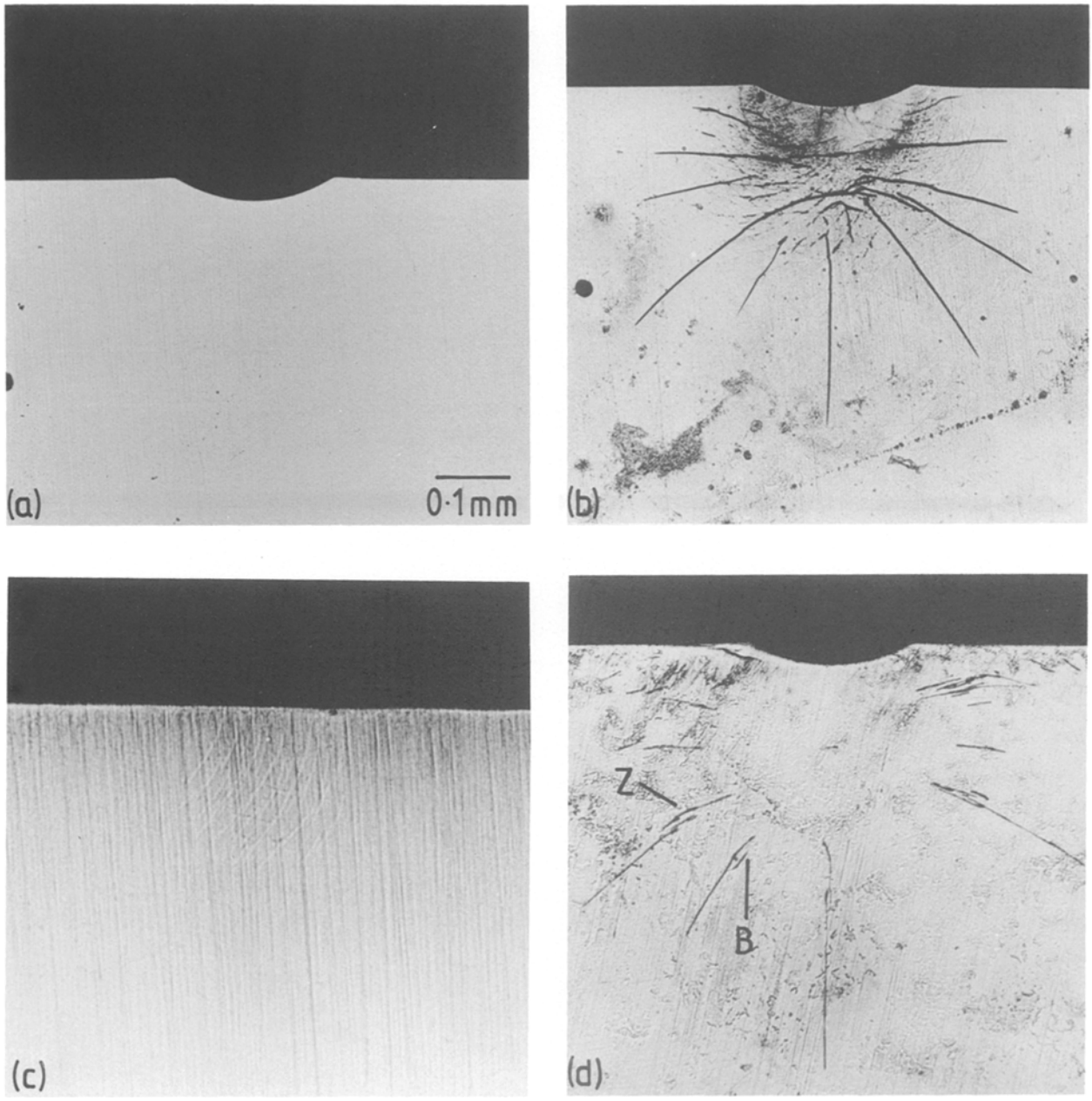

Figure 7 Vertical sections through a spherical indentation: (a) polished section before etching; (b) the same section after etching; (c) a section through the outer part of the surface plastic zone showing the curving Hartmann lines; (d) a section near the central symmetry plane of the indentation. Nomarski interference contrast.

(Fig. 8c) a lateral crack at "L" can be seen propagating towards the surface, apparently along a slip line. As in Fig. 7, the subsurface conical cracks follow the boundary of the plastic zone rather than passing right across it. Close to the edges of the plastic zone the cracks are split into groups of small cracks on approximately parallel planes.

5. Vickers indentations

The Vickers hardness, H_v obtained at a range of loads from 10 g to 10 kg was $538 \pm 16 . \mathrm{kg\,mm^{-2}}$, which agrees with the published value of Davis *et al.* [16]. Within experimental error this value was independent of load. As with the spherical indentations the ratio of hardness to compressive yield strength was 3.0, in agreement with both models of plastic indentation.

At applied loads of up to 50 g the indentations were featureless, with no sign of the characteristic coronets. These were first observed at a load of 100 g and when the load was increased to 1 kg the coronets became so prominent that the indentations developed the well-known distorted "barrel" outline which is characteristic of materials which pile up around the indentor [6].

Etching the indented specimens revealed cracks propagating from one or more corners of the indent provided that the load had exceeded 10 g. This is illustrated in Fig. 9d. At higher loads all four corner cracks developed and sometimes additional radial cracks propagated from the flat facets of the indentation. These extra radial cracks were usually associated with lateral cracks, as shown in Fig. 9a. Fig. 9b shows that, as with the spherical indents, below the surface the radial cracks start at the edge of the plastic zone rather than at the contact surface. Examination of subsequent horizontal sections showed that the plastic zone again extended deeper into the glass than did the radial cracks.

The only feature associated with the sharp Vickers

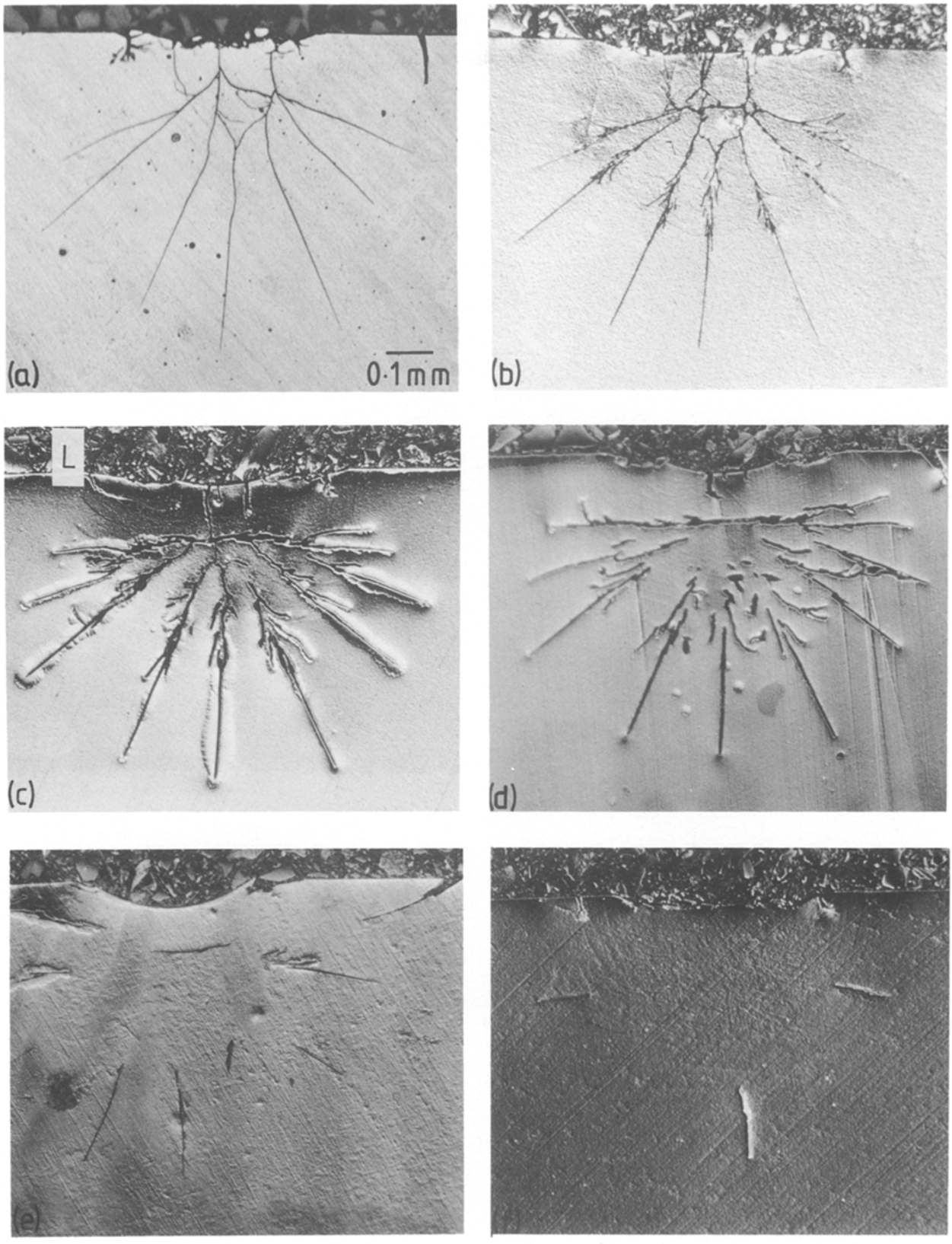

Figure 8 Vertical sections through a spherical indentation. The surface of this specimen was etched before sectioning and the traces of lateral and shallow radial cracks can be seen. Nomarski interference contrast.

indentor which was not observed in the case of the spherical indentor is shown in Fig. 9c. This indentation was formed at a load of 10 kg, the highest load used, and it can be seen that the inner part of one of the radial corner cracks is now visible at the surface before etching. After etching this crack would extend out to a distance of one to two times the indent diagonal.

Attempts were made to obtain a vertical section through a Vickers indentation but these were unsuccessful.

6. Discussion

6.1. Plastic flow

The spiral slip lines observed on the surface around a spherical indentation and in the subsurface plastic

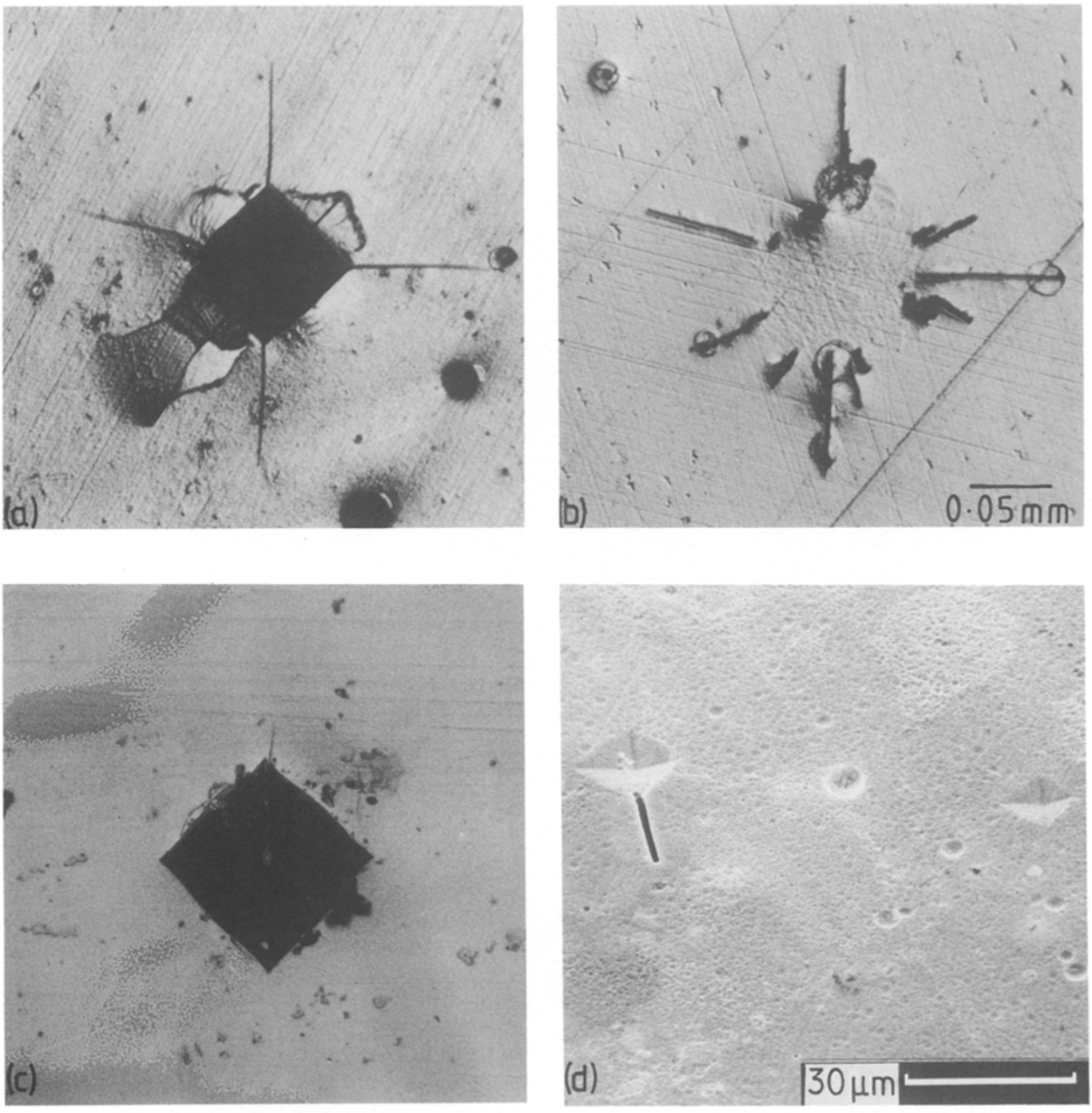

Figure 9 Vickers indentations: (a) surface appearance after etching; (b) sub-surface section through the same indent as (a); (c) an indentation produced at 10 kg load, before etching; (d) SEM image of 20 and 10 g indentations after etching, showing cracking at only the higher load.

zone beneath spherical and Vickers indentors are characteristic of the flow of material away from a central pressure [19]. Both this and the shape and appearance of the plastic zone, in which very few of the slip lines reach the free surface, indicate that Marsh's expanding cavity model of indentation is much more appropriate to this material than the rigid/plastic slipline field model. The appearance of the coronet pile-ups is thus misleading: they are not a necessary part of the deformation process, because they do not appear if the load is sufficiently small, and when they do appear at higher loads they are not particularly important, because, as can be seen from Fig. 7, their volume is negligible compared with the volume of the plastic zone. $Pd_{40}Ni_{40}P_{20}$ glass thus does obey the model which would have been expected from its low value of E/H and the formation of the coronets does not require a special explanation, as suggested previously [11].

It should be noted that even though the net movement of material is radial flow away from the indentor there is no evidence in this material for any direct radial flow analogous to the radial compaction which occurs in silicate glasses [7]. All the movement seems to be along the spiral slip lines which are approximately the trajectories of maximum shear stress, the radial movement being produced by slip first on one set of stress contours and then on the other, as illustrated schematically in Fig. 10. The form of the yield criterion (Equation 2) means that the slip lines will deviate from the contours of maximum shear stress towards the most tensile principal stress direction, and it can be seen from, for example, Fig. 6b that the slip lines do not in fact intersect one another at right-angles. However, too much weight should not be laid on this observation, firstly because elastic recovery on unloading will have affected the intersection angles and secondly because the shape of the plastic zone,

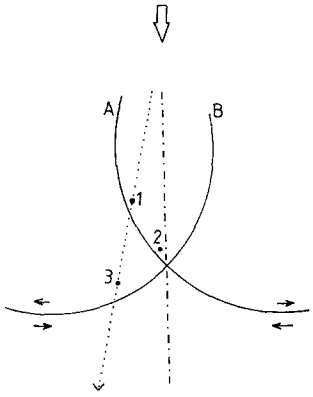

Figure 10 Schematic diagram showing radial movement produced by slip on two conjugate planes. Material at 1 is sheared firstly to position 2 by slip on A and then to position 3 by slip on B, producing net displacement in the direction of the dotted line.

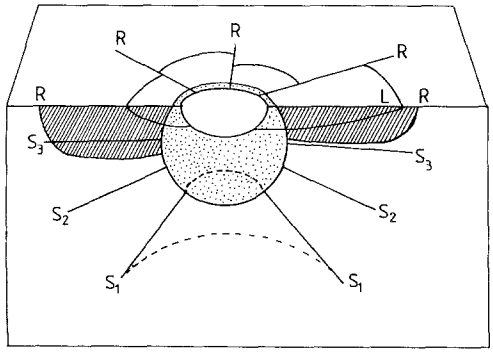

Figure 11 Simplified diagram showing the crack systems observed around spherical indentations. R, shallow radial cracks (system I) L, lateral cracks (system II), S, conical cracks (system III).

and hence the slip band angles, changes as the load increases and there is no guarantee that the intersecting slip-lines observed on the sections were active at the same time.

6.2. Fracture

The cracks observed around and beneath the indentations may be divided into three systems, each of which is analogous to a crack system produced in other materials during indentation. The first system, I, is the shallow radial cracks, which extend right into the contact zone near the free surface but follow the boundary of the plastic zone beneath the surface. This crack system is analogous to the "Palmqvist" radial crack system observed in, for example, silicate glasses, alumina and silicon carbide [20] and in tungsten carbide composites [21]. The second system, II, is the shallow lateral cracks, which are very commonly observed when brittle materials are indented and which form on unloading [18]. The third system, III, is the deeper, incomplete conical cracks which have approximately radial traces when observed on vertical sections. It should be emphasized that there is no evidence from sectioning either the Vickers or the spherical indentations for the development in this material of the penny-shaped median cracks, illustrated in Fig. 1a, which extend up to the free surface. The distribution of cracks around a spherical indent in $Pd_{40}Ni_{40}P_{20}$ metallic glass inferred from the horizontal and vertical sections is illustrated schematically in Fig. 11.

By analogy with other materials we may reason that the system III cracks, or incipient cracks, are likely to have formed during the loading cycle as the plastic zone expanded into and stretched the surrounding material. For all the indentations examined these cracks appear to emanate from the edge of the expanding plastic zone. This implies that as the load increased not only must the leading edges of these cracks have extended further into the elastic region, but that closure and healing of the cracks must have occurred at their trailing edges; otherwise we should still see these cracks extending back across the plastic zone towards the contact region, in the positions they must have occupied earlier in the loading cycle when the plastic zone was smaller. Indeed in Figs 7b and 8d, for example, short discontinuous segments of crack can be seen, particularly in the lower part of the plastic zone, which could be portions of former, partially healed cracks which have been displaced by subsequent slip. When these former cracks come into the high hydrostatic pressure at the core of the expanding plastic zone they are evidently entirely obliterated.

This model explains an otherwise puzzling observation, which is the splitting of the system I and III cracks into several short, approximately parallel segments at the boundary of the plastic zone (see, for example, Figs 5d and 8b). If these crack clusters formed independently their origin is not obvious, because the formation of one radial crack must relieve the tensile stress which was acting across it and there would then be no stress to nucleate a parallel crack in the immediate vicinity. However, if each crack cluster is formed by the shearing in three dimensions of a single original crack, with healing or perhaps further propagation of the sheared fragments, this difficulty does not arise. Such a displacement of part of a crack across a slip line in the outer part of a plastic zone, where the geometry of slip is still simple, can be seen in Fig. 6c.

It has been suggested that during the indentation of silicate glasses cracks may be nucleated at the intersection of two slip lines [18]. There is no evidence that this is occurring in $Pd_{40}Ni_{40}P_{20}$. From the above argument the short crack segments observed within the plastic zone would be interpreted as fragments of previously existing cracks, rather than new cracks being nucleated, and even in cases where a new crack appears to be forming at the edge of the plastic zone (e.g. Fig. 7d) it is not possible to be sure that this is really what is happening. Certainly many intersecting slip lines can be seen in the figures which are not associated with cracks at all.

The system I and II cracks do not penetrate the free surface, as is shown by the lack of surface movement, until the material is etched. It has been shown in ceramic materials that if the surface contains residual compressive stress, Palmqvist and lateral cracking are reduced or suppressed [22]. Because the specimens used in this investigation were prepared by mechanical polishing it is possible that this is the explanation here, but on the other hand Vickers indentations are often

made on the unprepared surfaces of as-quenched and stress-relieved metallic glass ribbons and although coronets are usually produced, which the results of this investigation suggest is an indication that the load should be high enough to induce Palmqvist corner cracks, cracks are not generally observed. It therefore seems more probable that the tensile stresses developed in the surface layers on unloading are not high enough to propagate these cracks as far as the surface, perhaps because plastic flow occurs differently in the less constrained surface layers and alters the form of the residual stress field. The acid etch then opens up the incipient cracks by stress-corrosion.

It seems probable, in fact, that all the cracks observed in these experiments are incipient rather than fully developed cracks until they are attacked by the acid. In the elastic region around an indentation the stress cannot by definition have exceeded the yield stress of the glass, so the observation of fully developed cracks in this region would imply that the fracture strength of the material must be less than its yield strength, i.e. that it is macroscopically brittle. However, $Pd_{40}Ni_{40}P_{20}$ glass may be deformed to high plastic strains in bending without any sign of cracking on the tension side of the bend, so that in bending it clearly behaves as a macroscopically ductile material. The presence of crack nuclei rather than developed cracks around the indentations would account for this apparent inconsistency and might also explain why the conical system III cracks observed on the vertical sections do not also etch up as ring cracks on horizontal sections: appreciable residual tensile stress across an incipient crack is probably required before it can be preferentially etched. Analysis of elastic/plastic indentations has shown that particularly high circumferential (hoop) tensile stresses may develop around the plastic zone on unloading, and these would tend to open incipient cracks radially, while the magnitude of the residual stress acting in the radial direction, which would tend to open circumferential cracks, is generally smaller [23].

In brittle materials measurements of the Palmqvist and median cracks are used to determine the fracture toughness [24]. In $Pd_{40}Ni_{40}P_{20}$ the median cracks are not developed into the full penny-shaped geometry necessary for this but it seems possible that a measurement might be obtained from the system I cracks. Accordingly, the mean crack length, c_0, was determined for the long radial surface cracks around the spherical indents after etching and the results are given in Table III. The scatter in crack lengths for each indent is rather large and it is not clear whether or not the shorter cracks should have been included as well, but the parameter $P/c_0^{2/3}$ is constant to within experimental error, as predicted by fracture mechanics theory [24]. The cracks around the Vickers indents could not be used because the full crack geometry was only developed around a few of the indents. The fracture toughness, K_c, estimated from the measurements given in Table III is $0.5\,MN\,m^{3/2}$, which is considerably smaller than the value of 10 to $20\,MN\,m^{3/2}$ which seems to be typical of metallic glasses [25]. This observation also suggests that the etch is revealing incipient crack nuclei rather than fully developed cracks. In any case, the validity of linear elastic fracture mechanics is extremely doubtful for such a plastic material.

TABLE III Surface radial cracks around spherical indentations

Load P (kN)	Mean crack length, c_0 (mm)	$P/(c_0)^{3/2}$ ($10^7\,Nm^{3/2}$)
0.359	0.65 ± 0.06	2.16 ± 0.25
0.290	0.45 ± 0.08	3.06 ± 0.65
0.140	0.28 ± 0.04	2.99 ± 0.50
0.100	0.26 ± 0.01	2.34 ± 0.13
0.050	0.16 ± 0.03	2.49 ± 0.58
0.030	0.10 ± 0.01	3.00 ± 0.40

It can now be seen that the changes in indent appearance described in Section 1 are part of a consistent picture. Coronet pile-ups at the free surface are formed only above a critical load, which is larger in the relatively soft $Pd_{40}Ni_{40}P_{20}$ glass than in the harder iron-based glasses. The suppression of coronets is annealed $Fe_{40}Ni_{40}P_{14}B_6$ glass [3] is thus simply correlated with the softening of the material at the beginning of crystallization, which is also displayed by the measured hardness values. The critical value of P/H for the formation of coronets in a Vickers test appears to be about 10^{-4}. On the other hand, the radial lines observed around Vickers indents after testing at low temperature [4] are almost certainly system I cracks which have reached the free surface, probably because the plastic flow in the surface layers which apparently hinders crack propagation at room temperature cannot occur at low temperature.

7. Conclusions

The response of $Pd_{40}Ni_{40}P_{20}$ glass to a spherical or pointed indentor involves both plastic flow and fracture. The geometry of slip and the form of the plastic zone appear to be broadly in agreement with the expanding cavity model of Marsh [7], but the net radial movement of material away from the indentor occurs by flow along slip lines which follow approximately, but because of the form of the yield criterion not exactly, the trajectories of maximum shear stress, rather than by direct radial flow or compaction. No work-hardening occurs during indentation.

The expansion of the growing plastic zone is accommodated by sub-surface cracking, or more probably incipient cracking, apparently on approximately conical surfaces in the elastically strained region around the indentation. As the plastic zone extends, the trailing edges of the cracks or incipient cracks are first displaced by slip and later closed by the compressive stress, so that they are always observed to emanate from near the elastic/plastic boundary. A similar process of local cracking would be expected to occur during rolling deformation and may have contributed to the decrease in density which has been reported in metallic glasses after rolling [26]. Further investigation of this is in progress. Shallow incipient radial and lateral crack systems are also formed around both Vickers and spherical indentations but do not penetrate to the free surface unless the material

is initially relatively brittle or the specimen is etched. The reason for this is thought to be that plastic flow at the free surface during loading alters the residual stress field present on unloading which leads to the formation of these cracks.

Acknowledgements

The author would like to thank T. Whitworth for experimental assistance, E, Yoffe and M. M. Chaudhri for helpful discussions, Professor D. Hull for the provision of laboratory facilities and the Royal Society for financial support.

References

1. F. DEN BROEDER and J. VAN DER BORST, *J. Appl. Phys.* **50** (1979) 4279.
2. L. A. DAVIS, *Scripta Metall.* **9** (1975) 431.
3. J. P. PATTERSON, A. L. GREER, J. A. LEAKE and D. R. H. JONES, in "Rapidly Quenched Metals III", Vol. 2, edited by B. Cantor (The Metals Society, London, 1978) p. 293.
4. C. A. PAMPILLO, *J. Mater. Sci.* **10** (1975) 1194.
5. P. E. DONOVAN, *Mater. Sci. Engng.* **97** (1988) 487.
6. D. TABOR, *Rev. Phys. Technol.* **1** (1970) 145.
7. D. M. MARSH, *Proc. Roy. Soc. (Lond.)* **A279** (1964) 420.
8. M. V. SWAIN and J. T. HAGAN, *J. Phys. D* **9** (1976) 2201.
9. J. T. HAGAN, *J. Mater. Sci.* **14** (1979) 462.
10. P. OSTOJIC and R. McPHERSON, *Int. J. Fracture* **33** (1987) 297.
11. P. M. SARGENT and P. E. DONOVAN, *Scripta Metall.* **16** (1982) 1207.
12. F. SPAEPEN, *Acta Metall.* **25** (1977) 407.
13. A. S. ARGON, *ibid.* **27** (1979) 47.
14. H. S. CHEN, *Scripta Metall.* **7** (1973) 931.
15. E. F. LAMBSON, W. A. LAMBSON, J. E. MacDONALD, M. R. J. GIBBS, C. A. SAUNDERS and D. TURNBULL, *Phys. Rev.* **B33** (1986) 2380.
16. L. A. DAVIS, C.-P. CHOU, L. E. TANNER and R. RAY, *Scripta Metall.* **10** (1976) 937.
17. L. HARTMANN, "Deformations dans les metaux" (Berger-Levrault, Paris, 1896).
18. J. T. HAGAN and M. V. SWAIN, *J. Phys. D.* **11** (1978) 2091.
19. A. NADAI and A. M. WAHL, "*Plasticity*" (McGraw-Hill, New York, 1931).
20. J. LANKFORD, *J. Mater. Sci.* **16** (1981) 1177.
21. M. T. LAUGIER, *J. Mater. Sci. Lett.* **6** (1987) 897.
22. T. HARANOH, H. ISHIKAWA, N. SHINKAI and M. MIZUHASHI, *J. Mater. Sci.* **17** (1982) 1493.
23. C. M. PERROTT, *Wear* **45** (1977) 293.
24. B. LAWN and R. WILSHAW, *J. Mater. Sci.* **10** (1975) 1049.
25. L. A. DAVIS, *Met. Trans.* **10A** (1979) 235.
26. R. W. CAHN, N. A. PRATTEN, M. G. SCOTT, H. R. SINNING and L. LEONARDSSON, in "Rapidly Solidified Metastable Materials", Materials Research Society Symposium Proceedings 28, edited by B. H. Kear and B. C. Giessen (North-Holland, New York, 1984) p. 241.

Received 26 January
and accepted 10 June 1988